# Perspectives on the reaction force constant

Peter Politzer · Jane S. Murray · Pablo Jaque

**Abstract** A synchronous, concerted chemical process is rigorously divided by the reaction force $\mathbf{F}(\mathbf{R})$, the negative gradient of $V(\mathbf{R})$, into "reactant" and "product" regions which are dominated by structural changes and an intervening "transition" region which is electronically intensive. The reaction force constant $\kappa(\mathbf{R})$, the second derivative of $V(\mathbf{R})$, is negative throughout the transition region, not just at the nominal transition state, at which $\kappa(\mathbf{R})$ has a minimum. This is consistent with experimental evidence that there is a transition *region*, not simply a specific point. We show graphically that significant nonsynchronicity in the process is associated with the development of a maximum of $\kappa(\mathbf{R})$ in the transition region, which increases as the process becomes more nonsynchronous. (We speculate that for a nonconcerted process this maximum is actually positive.) Thus, $\kappa(\mathbf{R})$ can serve as an indicator of the level of nonsynchronicity.

**Keywords** Reaction force · Reaction force constant · Synchronicity of chemical processes · Concertedness

## The reaction force and the reaction force constant

Consider a chemical process for which the variation of the potential energy $V(\mathbf{R})$ along the intrinsic reaction coordinate

P. Politzer (✉) · J. S. Murray
Department of Chemistry, University of New Orleans,
New Orleans, LA 70148, USA
e-mail: ppolitze@uno.edu

P. Politzer · J. S. Murray
CleveTheoComp, 1951 W. 26th Street, Suite 409,
Cleveland, OH 44113, USA

P. Jaque (✉)
Departamento de Ciencias Químicas, Facultad de Ciencias
Exactas, Universidad Andres Bello, Av. República 275,
Santiago, Chile
e-mail: pjaque@unab.cl

$\mathbf{R}$ has the familiar form shown in Fig. 1a. Whether the process is exothermic or endothermic is immaterial to this discussion. Figure 1a defines three key points on $\mathbf{R}$: the equilibrium reactants and products at A and B, and the maximum of $V(\mathbf{R})$ at β, commonly interpreted as the transition state. These allow the evaluation of the activation energy, $\Delta E_{act}$, and the net energy change, $\Delta E$:

$$\Delta E_{act} = V(\beta) - V(A) \tag{1}$$

$$\Delta E = V(B) - V(A). \tag{2}$$

However, a $V(\mathbf{R})$ plot contains a great deal more information that is not as immediately evident. One way to gain additional information from a curve is to look at its derivatives. In the case of $V(\mathbf{R})$, these actually have well-defined physical interpretations. From classical physics, the negative gradient of a potential energy is a force,

$$\mathbf{F}(\mathbf{R}) = -\partial \mathbf{V}(\mathbf{R})/\partial \mathbf{R}, \tag{3}$$

and the second derivative is a force constant,

$$\kappa(\mathbf{R}) = \partial^2 V(\mathbf{R})/\partial \mathbf{R}^2. \tag{4}$$

The analyses of $\mathbf{F}(\mathbf{R})$, the "reaction force," and $\kappa(\mathbf{R})$, the "reaction force constant," were pioneered by Toro-Labbé [1] and by Jaque et al. [2], respectively.

For the $V(\mathbf{R})$ in Fig. 1a, $\mathbf{F}(\mathbf{R})$ and $\kappa(\mathbf{R})$ are displayed in Fig. 1b and c. The points of inflection of $V(\mathbf{R})$ give rise to a minimum of $\mathbf{F}(\mathbf{R})$ at α and a maximum at γ. $\kappa(\mathbf{R})$ is positive in the regions prior to the $\mathbf{F}(\mathbf{R})$ minimum and after the $\mathbf{F}(\mathbf{R})$ maximum, and negative in the region between them; it has a minimum at the point β where $V(\mathbf{R})$ has its maximum.

How are $\mathbf{F}(\mathbf{R})$ and $\kappa(\mathbf{R})$ to be interpreted? Since $V(\mathbf{R})$ is the total energy of the reacting system at the point $\mathbf{R}$, $\mathbf{F}(\mathbf{R})$ is the resultant of all forces operating within it at that point. When $\mathbf{F}(\mathbf{R})$ is negative, it is opposite in direction to increasing $\mathbf{R}$ and is therefore opposing the process. Energy must be
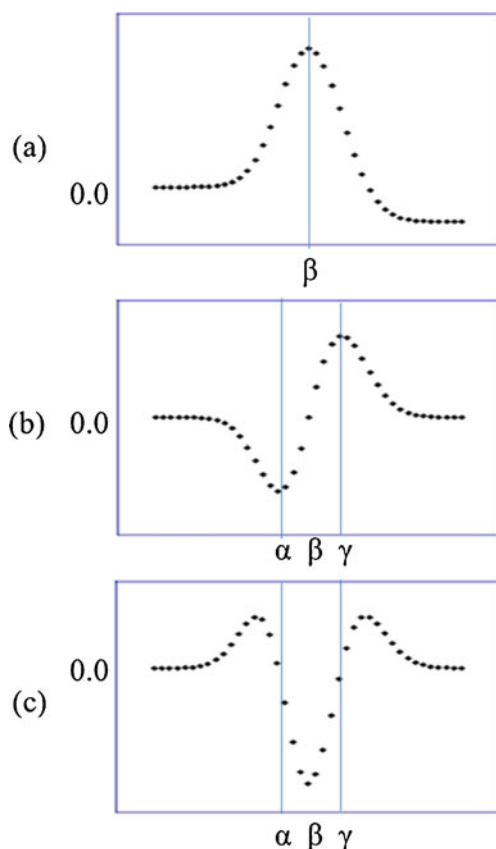
**Fig. 1a–c** Profiles of **a** $V(\mathbf{R})$, **b** $\mathbf{F}(\mathbf{R})$, and **c** $\kappa(\mathbf{R})$ along the intrinsic reaction coordinate $\mathbf{R}$ of a generic one-barrier reaction

provided to overcome this retarding force. When $\mathbf{F}(\mathbf{R})$ is positive, it is driving the reaction toward the products, and energy is being released. $\mathbf{F}(\mathbf{R})$ is zero at A and at B, where the reactants and products are at equilibrium, and it is zero at $\beta$, where $V(\mathbf{R})$ has a maximum.

$\kappa(\mathbf{R})$ indicates whether each increment in $\mathbf{R}$ will result in $\mathbf{F}(\mathbf{R})$ increasingly opposing or increasingly promoting the process. The maxima and minimum of $\kappa(\mathbf{R})$ are associated with the inflection points of $\mathbf{F}(\mathbf{R})$.

We wish to emphasize that the reaction force $\mathbf{F}(\mathbf{R})$ and the reaction force constant $\kappa(\mathbf{R})$ are not properties that have been defined or introduced for some purpose. They are intrinsic features of $V(\mathbf{R})$, and are rigorously and uniquely determined solely by $V(\mathbf{R})$. Our focus in this paper will be upon the significance of $\kappa(\mathbf{R})$, but we will begin by discussing both $\mathbf{F}(\mathbf{R})$ and $\kappa(\mathbf{R})$.

**Regions of a reaction**

Consider a process that has a $V(\mathbf{R})$ profile such as that in Fig. 1a. $\mathbf{F}(\mathbf{R})$ divides the intrinsic reaction coordinate into three regions, separated by the minimum and maximum of $\mathbf{F}(\mathbf{R})$: A → $\alpha$, $\alpha$ → $\gamma$, and $\gamma$ → B. Analysis

of an extensive series of reactions, cited by Murray et al. [3], has shown a consistent general pattern in what occurs in these regions [4, 5].

In the first "reactant" region, from A to $\alpha$, largely structural changes in the reactants take place: bond lengthening, angle bending, rotation, etc. These are preparation for the next phase of the reaction. For example, in the $S_N2$ substitution

$$H_3C - Cl + H_2O \rightarrow H_3C - OH + HCl, \qquad (5)$$

the main event between A and $\alpha$ was found to be a significant lengthening of the C–Cl bond [6]. Such structural alterations are resisted by the reaction force $\mathbf{F}(\mathbf{R})$, which is increasingly negative (retarding), reaching its greatest magnitude at $\alpha$. At this point, the system can be viewed as distorted (or activated) states of the reactants.

The second region, between $\alpha$ and $\gamma$, is primarily a transition to distorted products. It is here that electronic effects are most likely: new bonds forming, rapid and extensive variations in properties such as electrostatic potentials and local ionization energies, etc. In the reaction depicted in Eq. 5, it is between $\alpha$ and $\gamma$ that the C–Cl and O–H bonds break and the C–O and H–Cl bonds form [6]. $\mathbf{F}(\mathbf{R})$ now has an increasing positive component, which promotes and drives the transition. $\mathbf{F}(\mathbf{R})$ attains a maximum at $\gamma$, where the system can be regarded as distorted (or activated) states of the products.

In the final "product" region, $\gamma \rightarrow$ B, the distorted products relax structurally through bond length and angle changes, etc. $\mathbf{F}(\mathbf{R})$ is now a *positive* restoring force that drives the products to their final equilibrium states; it decreases in magnitude as these are approached.

The three regions can be characterized by the sign of $\kappa(\mathbf{R})$. It is positive in the structurally intensive reactant and product regions, and negative throughout the intervening transition to products.

We must emphasize that the preceding discussion has focused upon what have been found to be the dominant features of each of the three regions. It should not be inferred that there is no overlap. There will of course be some changes in the electronic density distribution (usually relatively minor and gradual) that accompany the structural effects in the reactant and product regions, and some structural changes (generally fairly small) in the transition region.

At least two other types of analysis lead to multi-region depictions of chemical reactions analogous to that presented here. Kraka and Cremer's "unified reaction valley approach," which is based upon the reaction path direction and curvature, involves a "preparation

phase," one or more "transition phases," in which bond breaking and formation take place, and a "product adjustment phase" [7].

On a more empirical level, there is "diabatic analysis," originally proposed by Marcus for modeling electron transfer processes [8]. This uses parabolas to represent the potential energy curves of the reactants and products, and accounts for the interaction by linking the parabolas. The portions before and after the link can be viewed as describing the structural changes in the reactant and product regions of the reaction, while the link corresponds to the transition region [9]. Somewhat in the same vein are the depictions of reactions presented by Evans and Polanyi [10] and by Dewar [11].

For a process that can be described by Fig. 1, the minimum of $\mathbf{F(R)}$ rigorously divides the activation energy into two components:

$$\begin{aligned} \Delta E_{\mathrm{act}} &= V(\beta) - V(\mathrm{A}) \\ &= [V(\alpha) - V(\mathrm{A})] + [V(\beta) - V(\alpha)] . \\ &= \Delta E_{\mathrm{act},1} + \Delta E_{\mathrm{act},2} \end{aligned} \quad (6)$$

$\Delta E_{\mathrm{act},1}$ is primarily the energy needed to overcome the resistance to the structural changes in the first region, A → $\alpha$, while $\Delta E_{\mathrm{act},2}$ is the energy required for the initial phase of the transition to products, $\alpha$ → $\beta$.

This decomposition of the activation energy can be very helpful in elucidating mechanistic questions, and in understanding the effect of a catalyst, solvent, or other external agent upon the reaction rate. By evaluating $\Delta E_{\mathrm{act},1}$ and $\Delta E_{\mathrm{act},2}$ both in the presence and the absence of the agent, it is possible to determine whether it mainly influences structural factors in the first region or electronic ones in the initial portion of the transition region. An extensive discussion of such applications of this activation energy decomposition is given by Politzer et al. [5].

There is also an interesting relationship to the Hammond–Leffler postulate [12, 13], according to which the transition state in an endothermic reaction more closely resembles the products and that in an exothermic reaction more closely resembles the reactants. Our experience has been that in an endothermic process, the structural changes in the first region, prior to $\alpha$, usually require more energy than is released in the relaxation in the third region, after $\gamma$ [9]; the reverse is true for an exothermic process. This can be viewed as a variation of the Hammond–Leffler postulate; however, the emphasis is not upon the transition state but rather upon the distorted reactants and products at the beginning and end of the transition region.

In another approach that has been used for partitioning $\Delta E_{\mathrm{act}}$, it is divided into (a) the energy needed for the reactants to assume the geometries that they have in the transition state at $\beta$ without interacting, and (b) the subsequent interaction energy between them [14–16]. While this is unrealistic (these are not two separate, independent events, as are the progressions from A to $\alpha$ and $\alpha$ to $\beta$), this approach should be comparable to Eq. 6 to the extent that the major structural changes do occur prior to $\alpha$.

## The reaction force constant

### The transition region

In the reactant and product regions of the process described by Fig. 1, $\mathbf{F(R)}$ can be viewed as a "restoring" force, in that it is directed toward bringing either the distorted reactants or the distorted products to their equilibrium states. The reaction force constants $\kappa(\mathbf{R})$ associated with these restoring forces are positive. (Stretching a diatomic molecule presents a simple example.)

Between the force minimum at $\alpha$ and its maximum at $\gamma$, however, the system cannot be described as distorted reactants or products; it is in transition from the former to the latter. Figure 1c shows that $\kappa(\mathbf{R})$ is now negative, not only at what has traditionally been labeled the transition state, at $\beta$, but throughout the region between $\alpha$ and $\gamma$; $\kappa(\mathbf{R})$ has a minimum at $\beta$.

Transition states have typically been characterized (and verified) by one (and only one) of the normal vibrational modes having an imaginary frequency—reflecting a negative force constant—at that point. The fact that the reaction force constant $\kappa(\mathbf{R})$ is negative throughout the entire transition-to-products portion of the process, from $\alpha$ to $\gamma$, suggests that it is more appropriate to refer to a transition region, defined by $\kappa(\mathbf{R}) < 0$, than a single transition state. This transition region is where the system goes from distorted reactants to distorted products; $\beta$ is simply one point in this region.

Zewail and Polanyi arrived at the concept of a transition region some time ago, via transition-state spectroscopy [17, 18]. They describe a continuum of transient, unstable states between perturbed forms of the reactants and products, which encompasses all bond breaking and formation. As we pointed out earlier [19], this continuum clearly corresponds to the transition region characterized by $\kappa(\mathbf{R}) < 0$; $\alpha$ and $\gamma$ are thus the boundaries of the continuum.

### Synchronous and nonsynchronous concerted reactions

The importance of recognizing that processes have transition *regions* rather than simply transition *states* becomes

evident, for example, in regard to synchronous and nonsynchronous concerted reactions. These involve two or more primitive processes (such as bond breaking and/or formation, rotation, etc.) with individual $V(\mathbf{R})$ profiles. The term "concerted" means that all of these processes take place in a single kinetic step, with no intermediates being involved [20]. Synchronous (nonsynchronous) indicates that the primitive processes proceed in unison (do not proceed in unison); e.g., the maxima of their $V(\mathbf{R})$ curves coincide (do not coincide).

We have recently computed $V(\mathbf{R})$, $\mathbf{F}(\mathbf{R})$, and $\kappa(\mathbf{R})$ for a series of concerted double proton transfer reactions [21, 22]. In most cases, the $V(\mathbf{R})$, $\mathbf{F}(\mathbf{R})$, and $\kappa(\mathbf{R})$ plots were qualitatively similar to those in Fig. 1. In a few instances, however, $\kappa(\mathbf{R})$ was notably different, especially in the transition region between $\alpha$ and $\gamma$. It was negative throughout this region, but instead of having one minimum, as in Fig. 1c, there was a local maximum, with minima on both sides of it.

It was suggested that this fine structure in $\kappa(\mathbf{R})$ in the transition region was indicative that the two proton transfers are considerably nonsynchronous [22] (i.e., two-stage processes) in Dewar's terminology [11]. When the proton transfers were fully or nearly fully synchronous, $\kappa(\mathbf{R})$ only had a minimum in the transition region, as in Fig. 1c. We will now present further support for this conjecture. (Note that "two-stage" is used to describe a highly nonsynchronous but still concerted reaction, whereas "two-step" means that a reaction is not concerted, but rather involves two kinetic steps with an intervening metastable intermediate.)

We will look at several model reactions, each involving two primitive steps (e.g., bond breaking and/or formation, etc.). These steps are described by potential curves $V_1(\mathbf{R})$ and $V_2(\mathbf{R})$; we assume that the total potential energy profile can be expressed by their sum,

$$V(\mathbf{R}) = V_1(\mathbf{R}) + V_2(\mathbf{R}), \qquad (7)$$

and that the total $\mathbf{F}(\mathbf{R})$ and $\kappa(\mathbf{R})$ curves are the corresponding sums
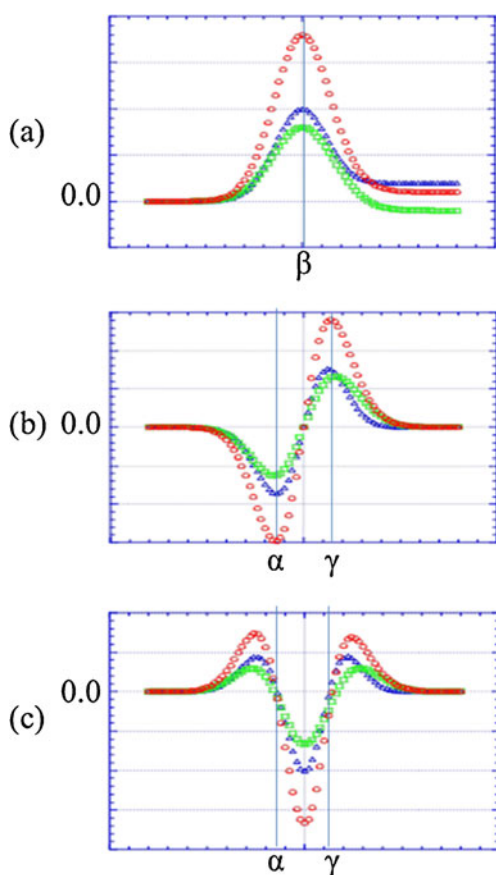


**Fig. 2** **a** Profiles of $V(\mathbf{R})$ in *red*, $V_1(\mathbf{R})$ in *blue*, and $V_2(\mathbf{R})$ in *green* along the intrinsic reaction coordinate $\mathbf{R}$ for a synchronous reaction. **b** Profiles of $\mathbf{F}(\mathbf{R})$ in *red*, $\mathbf{F}_1(\mathbf{R})$ in *blue*, and $\mathbf{F}_2(\mathbf{R})$ in *green*. **c** Profiles of $\kappa(\mathbf{R})$ in *red*, $\kappa_1(\mathbf{R})$ in *blue*, and $\kappa_2(\mathbf{R})$ in *green*
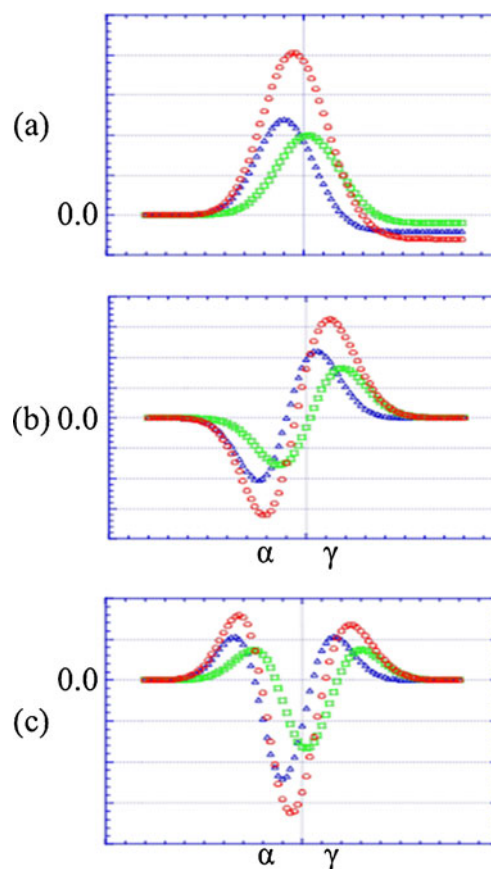


**Fig. 3** **a** Profiles of $V(\mathbf{R})$ in *red*, $V_1(\mathbf{R})$ in *blue*, and $V_2(\mathbf{R})$ in *green* along the intrinsic reaction coordinate $\mathbf{R}$ for a nearly synchronous reaction; $\beta_1$ and $\beta_2$ are separated by 1.2 units. **b** Profiles of $\mathbf{F}(\mathbf{R})$ in *red*, $\mathbf{F}_1(\mathbf{R})$ in *blue*, and $\mathbf{F}_2(\mathbf{R})$ in *green*. **c** Profiles of $\kappa(\mathbf{R})$ in *red*, $\kappa_1(\mathbf{R})$ in *blue*, and $\kappa_2(\mathbf{R})$ in *green*

$$\mathbf{F}(\mathbf{R}) = \mathbf{F}_1(\mathbf{R}) + \mathbf{F}_2(\mathbf{R}) \tag{8}$$

$$\kappa(\mathbf{R}) = \kappa_1(\mathbf{R}) + \kappa_2(\mathbf{R}). \tag{9}$$

$V_i(\mathbf{R})$, $\mathbf{F}_i(\mathbf{R})$, and $\kappa_i(\mathbf{R})$ were obtained by applying formulae derived by Labet et al. [23], in slightly modified forms:

$$\text{For } \mathbf{R} < \beta, \quad V(\mathbf{R}) = \Delta E_{act} \exp\left[\frac{-(\mathbf{R}-\beta)^2}{\lambda}\right] \tag{10}$$

$$\text{For } \mathbf{R} > \beta, \quad V(\mathbf{R}) = \Delta E + (\Delta E_{act} - \Delta E) \exp\left[\frac{-(\mathbf{R}-\beta)^2}{\lambda(1-\Delta E/\Delta E_{act})}\right]. \tag{11}$$

In Eqs. 10 and 11, $\beta$ is the point at which $V(\mathbf{R})$ has its maximum, $\Delta E_{act}$ is the activation energy (see Eq. 1), $\Delta E$ is the total change in energy (see Eq. 2), and $\lambda$ is a positive parameter related to the width of the activation barrier. By assigning different values to $\beta$, $\Delta E_{act}$, $\Delta E$

and $\lambda$, a variety of potential energy profiles $V_i(\mathbf{R})$ can be produced. The corresponding $\mathbf{F}_i(\mathbf{R})$ and $\kappa_i(\mathbf{R})$ can be determined by taking the derivatives of Eqs. 10 and 11 [23], as per Eqs. 3 and 4.

Figure 2 shows a fully synchronous concerted reaction: $V_1(\mathbf{R})$ and $V_2(\mathbf{R})$ were defined to have their maxima at the same point $\mathbf{R} = \beta$. The resulting $V(\mathbf{R})$, $\mathbf{F}(\mathbf{R})$, and $\kappa(\mathbf{R})$ curves are very much like those in Fig. 1. Even when the reaction is slightly nonsynchronous, such that the $V_1(\mathbf{R})$ and $V_2(\mathbf{R})$ maxima are separated but are still quite close to each other (Fig. 3), $V(\mathbf{R})$, $\mathbf{F}(\mathbf{R})$, and $\kappa(\mathbf{R})$ are still essentially similar to Fig. 1. In particular, $\kappa(\mathbf{R})$ has only a single minimum in the transition region. Figure 1 can evidently represent a single primitive process or a concerted, synchronous, or nearly synchronous reaction.
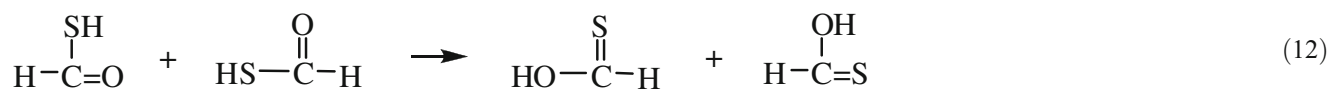
Our studies of double proton transfers, all of which were concerted, provide examples of both full and near-synchronicity [21, 22]. Full synchronicity was seen for perfectly symmetric reactions (identical molecules breaking and forming identical bonds), e.g.,
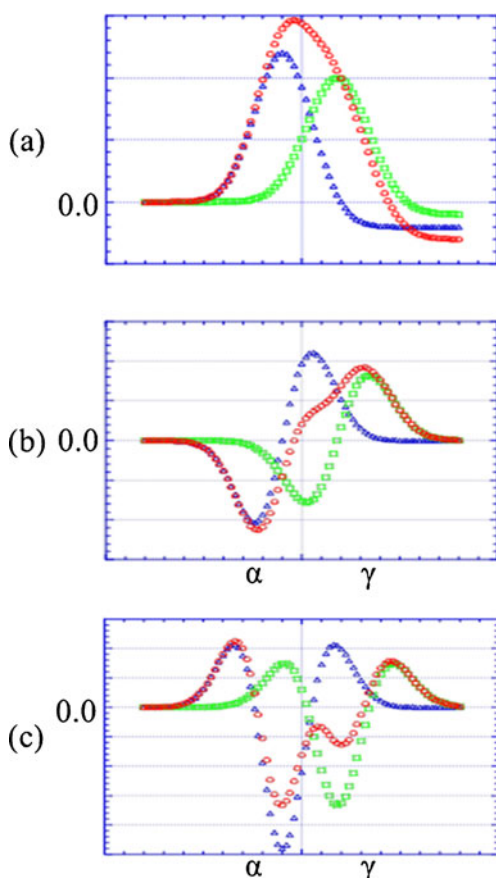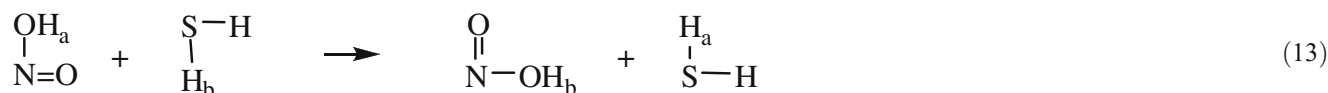


**Fig. 4** **a** Profiles of $V(\mathbf{R})$ in *red*, $V_1(\mathbf{R})$ in *blue*, and $V_2(\mathbf{R})$ in *green* along the intrinsic reaction coordinate $\mathbf{R}$ for a nonsynchronous reaction; $\beta_1$ and $\beta_2$ are separated by 2.8 units. **b** Profiles of $\mathbf{F}(\mathbf{R})$ in *red*, $\mathbf{F}_1(\mathbf{R})$ in *blue*, and $\mathbf{F}_2(\mathbf{R})$ in *green*. **c** Profiles of $\kappa(\mathbf{R})$ in *red*, $\kappa_1(\mathbf{R})$ in *blue*, and $\kappa_2(\mathbf{R})$ in *green*
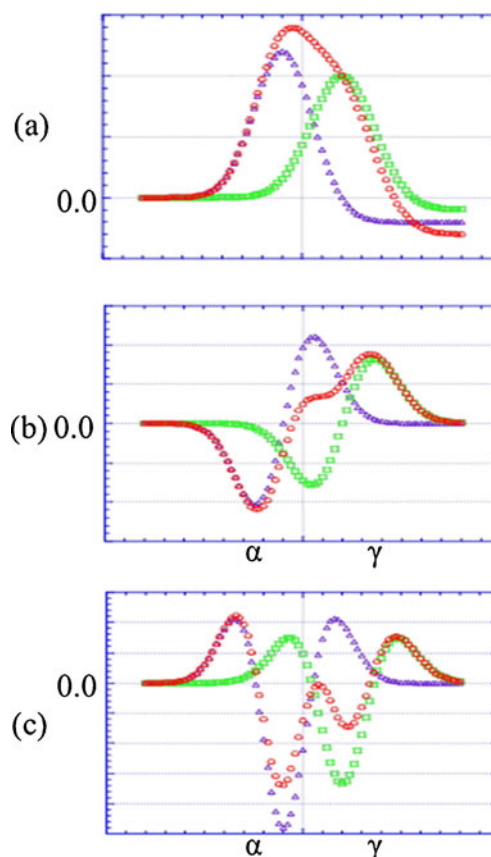


**Fig. 5** **a** Profiles of $V(\mathbf{R})$ in *red*, $V_1(\mathbf{R})$ in *blue*, and $V_2(\mathbf{R})$ in *green* along the intrinsic reaction coordinate $\mathbf{R}$ for a nonsynchronous reaction; $\beta_1$ and $\beta_2$ are separated by 3.0 units. **b** Profiles of $\mathbf{F}(\mathbf{R})$ in *red*, $\mathbf{F}_1(\mathbf{R})$ in *blue*, and $\mathbf{F}_2(\mathbf{R})$ in *green*. **c** Profiles of $\kappa(\mathbf{R})$ in *red*, $\kappa_1(\mathbf{R})$ in *blue*, and $\kappa_2(\mathbf{R})$ in *green*

$$\underset{\text{H}-\text{C}=\text{O}}{\overset{\text{SH}}{\vert}} \quad + \quad \underset{\text{HS}-\text{C}-\text{H}}{\overset{\text{O}}{\parallel}} \quad \longrightarrow \quad \underset{\text{HO}-\text{C}-\text{H}}{\overset{\text{S}}{\parallel}} \quad + \quad \underset{\text{H}-\text{C}=\text{S}}{\overset{\text{OH}}{\vert}} \tag{12}$$

Near-synchronicity was shown by, for instance, the $H_2S$-assisted double proton transfer,

$$\underset{\text{N}=\text{O}}{\overset{\text{OH}_a}{\vert}} \quad + \quad \underset{\text{H}_b}{\overset{\text{S}-\text{H}}{\vert}} \quad \longrightarrow \quad \underset{\text{N}-\text{OH}_b}{\overset{\text{O}}{\parallel}} \quad + \quad \underset{\text{S}-\text{H}}{\overset{\text{H}_a}{\vert}} \tag{13}$$

In contrast, Fig. 4 depicts a concerted process that is considerably nonsynchronous (i.e., two-stage); the maxima of $V_1(\mathbf{R})$ and $V_2(\mathbf{R})$ are markedly separate. The effect of this upon $V(\mathbf{R})$ is barely noticeable, and $\mathbf{F}(\mathbf{R})$ has just a small shoulder. H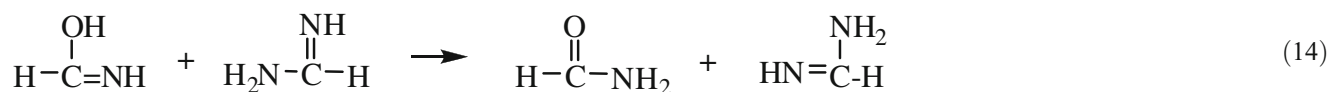owever, $\kappa(\mathbf{R})$, although still negative in the entire region between the minimum and maximum of $\mathbf{F}(\mathbf{R})$, now has a very distinct maximum between two minima. In Fig. 5, the process is yet more nonsynchronous, although still concerted, and the $\kappa(\mathbf{R})$ maximum has increased to almost zero. (In Figs. 3, 4 and 5, we do not show a point β for the potential energy curves, since the maxima of $V_1(\mathbf{R})$ and $V_2(\mathbf{R})$ do not coincide.) An example of a two-stage quite nonsynchronous double proton transfer is shown below [22]:
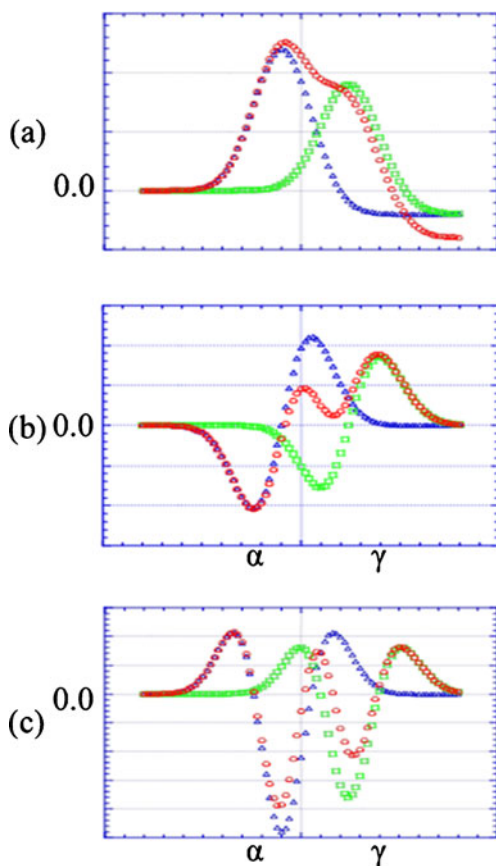


Fig. 6 **a** Profiles of $V(\mathbf{R})$ in *red*, $V_1(\mathbf{R})$ in *blue*, and $V_2(\mathbf{R})$ in *green* along the intrinsic reaction coordinate **R** for a nonsynchronous reaction; β$_1$ and β$_2$ are separated by 3.4 units. **b** Profiles of $\mathbf{F}(\mathbf{R})$ in *red*, $\mathbf{F}_1(\mathbf{R})$ in *blue*, and $\mathbf{F}_2(\mathbf{R})$ in *green*. **c** Profiles of $\kappa(\mathbf{R})$ in *red*, $\kappa_1(\mathbf{R})$ in *blue*, and $\kappa_2(\mathbf{R})$ in *green*
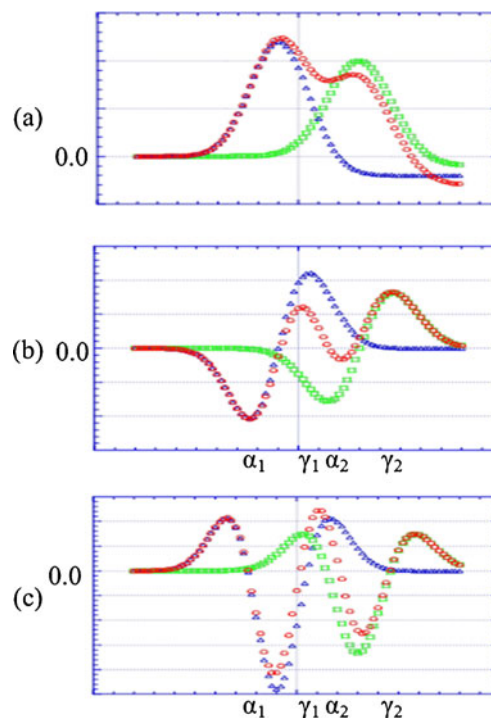


Fig. 7 **a** Profiles of $V(\mathbf{R})$ in *red*, $V_1(\mathbf{R})$ in *blue*, and $V_2(\mathbf{R})$ in *green* along the intrinsic reaction coordinate **R** for a two-barrier reaction; β$_1$ and β$_2$ are separated by 4.0 units. **b** Profiles of $\mathbf{F}(\mathbf{R})$ in *red*, $\mathbf{F}_1(\mathbf{R})$ in *blue*, and $\mathbf{F}_2(\mathbf{R})$ in *green*. **c** Profiles of $\kappa(\mathbf{R})$ in *red*, $\kappa_1(\mathbf{R})$ in *blue*, and $\kappa_2(\mathbf{R})$ in *green*. α$_1$ and γ$_1$ correspond to $V_1(\mathbf{R})$ (*blue curves*); α$_2$ and γ$_2$ correspond to $V_2(\mathbf{R})$ (*green curves*)

$$\underset{\text{H}-\overset{\overset{\text{OH}}{\|}}{\text{C}}=\text{NH}}{} \quad + \quad \underset{\text{H}_2\text{N}-\overset{\overset{\text{NH}}{\|}}{\text{C}}-\text{H}}{} \quad \longrightarrow \quad \underset{\text{H}-\overset{\overset{\text{O}}{\|}}{\text{C}}-\text{NH}_2}{} \quad + \quad \underset{\text{HN}=\overset{\overset{\text{NH}_2}{\|}}{\text{C}}\text{-H}}{} \tag{14}$$

Figures 4 and 5 demonstrate that fine structure in $\kappa(\mathbf{R})$ in the transition region does serve as an indicator of a nonsynchronous two-stage process, although its absence does not guarantee full synchronicity, as has been discussed previously [22] and can be seen in Fig. 3. It should be noted that $\kappa(\mathbf{R})$ is much more sensitive to nonsynchronicity than either $V(\mathbf{R})$ or $\mathbf{F}(\mathbf{R})$; the consequences of nonsynchronicity for $V(\mathbf{R})$ may be almost imperceptible—see Figs. 4a and 5a—and may simply be a shoulder in $\mathbf{F}(\mathbf{R})$—see Figs. 4b and 5b.

### Discussion and summary

If a concerted reaction is sufficiently nonsynchronous as to produce a shoulder between the minimum and maximum of $\mathbf{F}(\mathbf{R})$, as in Figs. 4b and 5b, then the separation of the $\mathbf{F}_i(\mathbf{R})$ curves of the primitive steps is enough that there is likely to be some overlap of a structurally intensive region of one with the electronically intensive region of another. In Fig. 5b, for instance, the second region defined by $\mathbf{F}_1(\mathbf{R})$ coincides with the first region defined by $\mathbf{F}_2(\mathbf{R})$. Thus, the concept of the overall reaction having reactant, transition, and product regions becomes less clear-cut as the reaction becomes more nonsynchronous.

When shoulders are created in the total $\mathbf{F}(\mathbf{R})$, additional points of inflection arise, and these result in new minima and maxima in $\kappa(\mathbf{R})$ in the region between the $\mathbf{F}(\mathbf{R})$ minimum and maximum. The presence of such fine structure in $\kappa(\mathbf{R})$ is accordingly an indicator of a significant level of nonsynchronicity (two or more stages); a very small degree of nonsynchronicity does not manifest itself as a shoulder in $\mathbf{F}(\mathbf{R})$, Fig. 3b, so there is no fine structure in $\kappa(\mathbf{R})$; see Fig. 3c.

Regardless of the level of nonsynchronicity, the $\mathbf{F}(\mathbf{R})$ and $\kappa(\mathbf{R})$ in Figs. 2, 3, 4, and 5 have certain key features in common: $\mathbf{F}(\mathbf{R})$ is initially negative and decreases to a minimum at $\alpha$; then it increases to a positive maximum at $\gamma$, possibly with a shoulder; and finally it diminishes to zero at the products. $\kappa(\mathbf{R})$ has positive maxima before $\alpha$ and after $\gamma$, and is negative everywhere between $\alpha$ and $\gamma$, with at least one minimum and possibly additional fine structure.

If we now separate the maxima of $V_1(\mathbf{R})$ and $V_2(\mathbf{R})$ a bit more (Fig. 6), we find significant *qualitative* changes, particularly in $\mathbf{F}(\mathbf{R})$ and $\kappa(\mathbf{R})$. While $V(\mathbf{R})$ gains a pronounced shoulder, $\mathbf{F}(\mathbf{R})$ has an additional minimum and maximum between $\alpha$ and $\gamma$, and $\kappa(\mathbf{R})$ has a maximum between $\alpha$ and $\gamma$ that *becomes positive*. These new features of $\mathbf{F}(\mathbf{R})$ and $\kappa(\mathbf{R})$ are further emphasized in Fig. 7, in which the maxima of $V_1(\mathbf{R})$ and $V_2(\mathbf{R})$ are far enough apart that $V(\mathbf{R})$ has acquired a second maximum. Figure 7 clearly represents a nonconcerted process, with an intermediate between two kinetic steps. However, one might speculate that the process in Fig. 6 should already be viewed as nonconcerted; the existence of a second kinetic step being revealed by the additional minimum and maximum in $\mathbf{F}(\mathbf{R})$, and especially by the positive maximum of $\kappa(\mathbf{R})$ in the region between $\alpha$ and $\gamma$. These speculations are being investigated.

The issues of concertedness vs. nonconcertedness and synchronicity vs. nonsynchronicity are of continuing interest in a variety of important reactions, such as Diels–Alder cycloadditions [11, 16, 24–27]. We are currently examining the features of $\kappa(\mathbf{R})$ in a series of Diels–Alder processes.

### References

1. Toro-Labbé A (1999) J Phys Chem A 103:4398–4403
2. Jaque P, Toro-Labbé A, Politzer P, Geerlings P (2008) Chem Phys Lett 456:135–140
3. Murray JS, Lane P, Göbel M, Klapötke TM, Politzer P (2009) Theor Chem Acc 124:355–363
4. Toro-Labbé A, Gutiérrez-Oliva S, Murray JS, Politzer P (2007) Mol Phys 105:2619–2625
5. Politzer P, Toro-Labbé A, Gutiérrez-Oliva S, Murray JS (2012) Adv Quantum Chem 64:189–209
6. Politzer P, Burda JV, Concha MC, Lane P, Murray JS (2006) J Phys Chem A 110:756–761
7. Kraka E, Cremer D (2010) Acc Chem Res 43:591–601
8. Marcus RA, Sutin N (1985) Biochim Biophys Acta 811:265–322
9. Politzer P, Reimers JR, Murray JS, Toro-Labbé A (2010) J Phys Chem Lett 1:2858–2862
10. Evans MG, Polanyi M (1938) Trans Faraday Soc 34:11–23
11. Dewar MJS (1984) J Am Chem Soc 106:209–219
12. Leffler JE (1953) Science 117:340–341
13. Hammond GS (1955) J Am Chem Soc 77:334–338
14. Nagase S, Morokuma K (1978) J Am Chem Soc 100:1666–1672
15. Bickelhaupt FM (1999) J Comput Chem 20:114–128
16. Ess DH, Houk KN (2008) J Am Chem Soc 130:10187–10198
17. Polanyi JC, Zewail AH (1995) Acc Chem Res 28:119–132
18. Zewail AH (2000) J Phys Chem A 104:5660–5694

19. Toro-Labbé A, Gutiérrez-Oliva S, Murray JS, Politzer P (2009) J Mol Model 15:707–710
20. Carey FA, Sundberg RJ (1984) Advanced organic chemistry, part A: structure and mechanisms, 2nd edn. Plenum, New York
21. Yepes D, Murray JS, Santos JC, Toro-Labbé A, Politzer P, Jaque P (2012) J Mol Model. doi:10.1007/s00894-012-1475-3
22. Yepes D, Murray JS, Politzer P, Jaque P (2012) Phys Chem Chem Phys 14:11125–11134
23. Labet V, Morell C, Toro-Labbé A, Grand A (2010) Phys Chem Chem Phys 12:4142–4151
24. Sauer J, Sustmann R (1980) Angew Chem Int Ed 19:779–807
25. Houk KN, González J, Li Y (1995) Acc Chem Res 28:81–90
26. Xu L, Doubleday CE, Houk KN (2010) J Am Chem Soc 132:3029–3037
27. Moyano A, Rios R (2011) Chem Rev 111:4703–4832